APPLICATION OF A MODIFIED PHASE DIAGRAM TO THE PRODUCTION OF

CAST ALLOY 718 COMPONENTS

G. K. Bouse Howmet Corporation Technical Center Whitehall, MI 49461

INTRODUCTION

The need for improved methods of thermal processing cast Alloy 718 continues to be a challenge because of its extensive use in the aerospace industry. It's many applications demand an ever increasing ultimate tensile strength, at least 1240 MPa (180 ksi) at room temperature [1]. These high tensile properties can be attained with a combination of fine grain size, proper homogenization, hot isostatic pressing (HIP), solution heat treatment, and aging if the metallurgy of the cast component is understood.

The formation (or suppression) of Laves' phase is an important aspect of cast Alloy 718 metallurgy. This Cb-rich phase develops during solidification, and like most segregated phases, segregates more with slower cooling rates. The presence of Laves' phase causes at least three different problems. First, the presence of Laves' phase depletes the potential of γ " precipitate strengthening, since Cb is also found in γ ". Second, Laves' phase melts at a temperature lower than that of the matrix, often producing incipient melting and porosity during high temperature processing. Third, Laves' phase represents a microstructural weakness in that decohesion under a tensile stress will often occur at the Laves'/matrix interface.

For the first twenty years, Eiselstein's [2] pseudo-binary phase diagram provided the metallurgist with a clue as to how the alloy was supposed to act. However, the diagram was largely ignored because production processes seldom permit the time required for equilibrium conditions to become established. This was unfortunate because with the exception of a few refinements, Eiselstein's diagram was remarkably accurate. With a more complete understanding of his diagram the use of cast Alloy 718 would probably be even more widespread than it is today.

In the current work, the author used precisely controlled heat treatments to determine the solidus and liquidus temperatures of cast Alloy 718. Quantitative metallography, electron microprobe analyses, and an application of the Lever Rule [3] were used to develop phase boundaries built upon Eiselstein's original work. In addition, recent efforts by Prinz and Rudolph [4] and Knorovsky and Cieslak et. al. [5] were incorporated which led to an improvement of the Alloy 718 pseudo-binary phase diagram. The improved diagram was used to explain problems encountered during heat treating and hot isostatic pressing (HIP) of Alloy 718 investment castings as well as Alloy 718 welds. Finally, DTA thermograms were presented and discussed in the Appendix which compliments our total understanding of the cast Alloy 718 physical metallurgy.

Superalloy 718—Metallurgy and Applications Edited by E.A. Loria The Minerals, Metals & Materials Society, 1989

TECHNICAL APPROACH

Material. The material chosen for study was Microcast-X® Alloy 718 [6], having a grain size of ASTM 3, and composition as listed in Table I. The as-cast material came from a mold holding sixteen 16 mm (5/8 inch) diameter bars. All of the samples came from the central portion of one bar. No other thermal cycling was performed on the cast bars. The structure resulting from Microcast-X processing exhibited a fine grained, nondendritic appearance.

Melting Chambers. Nineteen experiments were performed using two different furnaces. One furnace used the Perkin-Elmer (P-E) 1700 DTA cell. For the purpose of these experiments, the DTA system was only used to heat-up and hold the sample at temperature. The ~100 mg sample was heated in ultra high purity He at 20C/minute (35F/min.) up to the holding temperature, in the range of 1180-1330C (2150-2425F). The temperature was held for 15 minutes before furnace cooling at ~40C/minute (70F/min.). The precision of this system, using Pt-Rh thermocouples, was determined to be better than $\pm 5C$ ($\pm 10F$). The P-E cell was calibrated by melting Ni (>99.99% purity) at 1455C (2650F).

The other chamber used for the remaining eight experiments was a Centorr sessile drop vacuum furnace. The samples consisted of ~5 mm (0.25 in.) cubes, polished with metallographic papers. A W-Re thermocouple was adjusted so that it was within ~2 mm (0.08 in.) above the cube. The furnace was ramped at ~3C/minute (6F/min) near the test temperature and held for 15 minutes before furnace cooling at ~40C/minute (70 F/min). Calibration of the system was performed by observing when a commercially pure Ni pellet (ground as above into a 5 mm cube) completely melted to the bead shape. The precision of the Centorr furnace was estimated to be $\pm 10C$ ($\pm 18F$).

Quantitative Metallography (QM). Samples were metallographically prepared from both the P-E and Centorr runs. The melted areas were outlined manually between 100-200X using transparencies, which were then interpreted by a Leitz TAS Plus Image Analyzer. This was performed with three fields before

TABLE I ~	Alloy 718 Bulk,	Matrix, Interme	diate Region
	and Laves' Compo	ositions - Weigh	t Percent

	<u>_c</u>	<u>Cr</u>	<u>Fe</u>	Cb	Mo	<u>Ti</u>	<u>Al</u>	Si	<u>Ni</u>
Bulk Casting+							0.56 (± .01)		
Matrix (γ) Near Dendrite Center							0.5 (±0.1)		54.0 (±0.8)
Matrix (γ) Near Inter- mediate Region	nd						0.6 (±0.1)		55.2 (±0.6)
Intermediate Region	nd						0.6 (±0.1)		52.6 (±0.7)
Globular Laves'	nd						0.2 (±0.1)		
Eutectic Laves'	nd						0.3 (±0.1)		44.2 (±3.6)

⁺ Determined by wet and spectographic techniques; all others EMP analyses. nd Not determined.

^() Typical 1 sigma standard deviation based on multiple point analyses.

averaging to achieve the result. The melted regions usually consisted of Laves' phase, surrounded by an "intermediate" region - both of these areas were counted as having melted. When bulk melting occurred (resulting in a dendritic structure upon cooling), these results were averaged with the area fraction of micro-melted regions (if applicable) to achieve the percent melting. The precision of this technique was estimated to produce results within 1% melting.

Microprobe. A fully computer automated Cameca Camebax electron microprobe (EMP) was used to determine the chemical composition of the phases. Three to five analyses within each region were averaged for the reported result. The diameter of the EMP beam was ~l μm .

RESULTS AND DISCUSSION

Fractional Melting

Microstructures of the Microcast-X Alloy 718 in various stages of melting are shown in Figure 1. First, the Cb-rich liquid phase forms on the grain boundaries followed by liquation within the grains. With the cooling rates employed, the liquid phase had adequate time to form globular Laves' phase and an intermediate region that envelopes the Laves' phase. This intermediate region has a composition between that of Laves' and the matrix. In a few cases, the Laves' formed a eutectic which was also surrounded by this intermediate region. Examples of the globular and eutectic Laves' phase are shown in Figure 2.

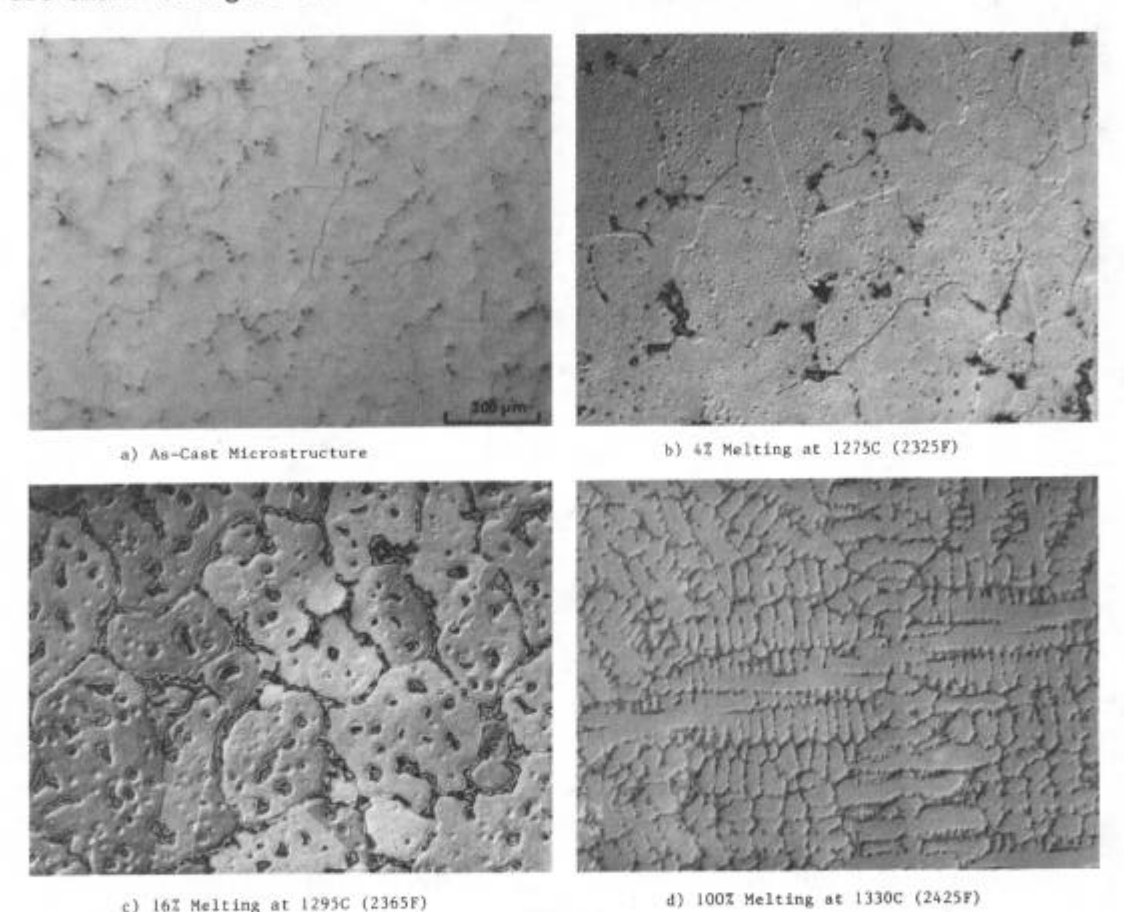


Figure 1. As-cast Microcast-X® Alloy 718 in (a), and at different temperatures within the melting range.

The micro-melting continued in increasing amounts until the entire sample melts (bulk melting). Bulk melting was characterized by the formation of dendrites upon cooling. Some of the liquation is also presumed to be caused by melting of the Cb carbides. Since the fraction of carbides was probably less than about 1.5% [7], the area fraction was ignored.

Results of the melting experiments are plotted in Figure 3. A linear regression of both Centorr and P-E data containing <30% melting yielded a solidus of 1254C (2290F), however, a more conservative value for the solidus temperature would be 1240C (2265F); the same as in [4]. The liquidus temperature for both Centorr and P-E data were determined to be 1330C (2425F), compared to 1340C (2445F) determined by [4]. Considering the two different heats between this study and [4], a 10C (18F) difference in the liquidus temperature could be due to minor differences in the heat chemistries or experimental techniques.

Note that the incipient melting point, usually observed at 1180C (2150F) was not detected. This is because there was practically no Laves' phase (<0.5%) to begin with, at least in the casting chosen for analysis. Even if there were melting, this amount would be difficult to detect metallographically at least by the QM techniques chosen. It was perhaps unusual that so little Laves' was in the samples, as 2-5% Laves' phase would be typical for production castings.

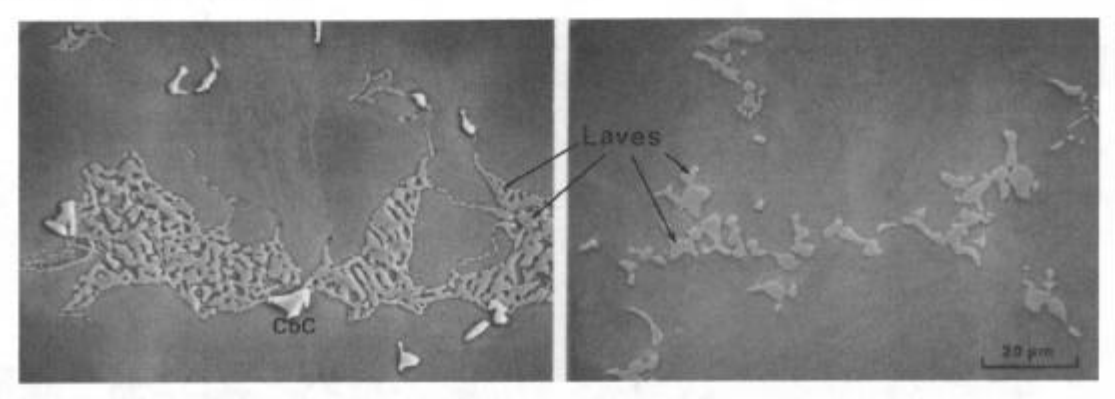


Figure 2. Examples of eutectic Laves' (left), and globular Laves' phase.

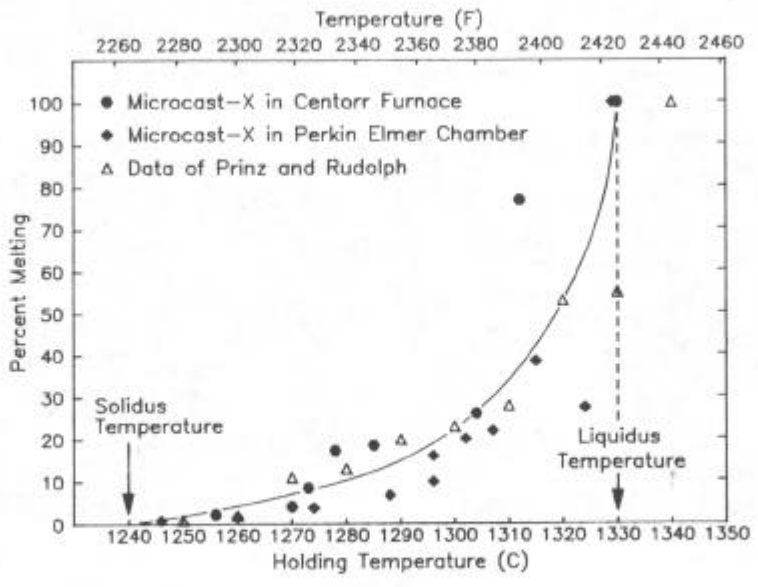


Figure 3. The percent melting versus holding temperature for samples run in Perkin-Elmer and Centorr furnaces. Data of [4] also included.

Phase Analyses

The phases that were analyzed came from two Centorr specimens that had been melted in the range of 1312-1330C (2394-2425F). Differences in reported chemistries between the two samples were within the 1 sigma error of measurement, and therefore the differences were determined to be insignificant.

Composition of Laves'. The exact amount of Cb in Laves' phase has been the subject of many discussions. In previous work on cast Alloy 718 components by the author using EMP techniques [7], ~28% Cb was found in globular Laves' much like values of ~30% Cb in globular Laves' recorded here. Reference [5] recorded a value of 22.4% Cb in Laves' using rapidly chilled weld metal and micro-analytical electron microscopy (AEM) techniques. In that study, a lamellar Laves' was observed and the possible influence of dissolved Cb carbides was positively eliminated. For this reason, 22.4% Cb was accepted as the composition of Laves' for purposes of the phase diagram.

When the eutectic Laves' was analyzed, only ~25% Cb was found. The eutectic Laves' is believed to have formed below the eutectic temperature, and therefore is subject to less diffusion. The composition of Laves' will probably continue to fluctuate depending upon the ability of the researcher to document the phase before significant diffusion occurs.

Composition of Matrix. The first solid that forms (γ , the centers of the cells or dendrites) rejects Cb, Mo, Ti, and Si, and attracts Al, Cr, Fe, and Ni. This γ has only ~2.5% Cb initially, increasing to only ~3.6% Cb. Eutectic γ analysis was attempted, however, the EMP beam diameter of ~1 μ m was too large to avoid picking up some of the neighboring Laves' phase. The lamellar eutectic γ determined by [5] provided a value of 9.3% Cb. For reasons described above, this value was accepted as the maximum Cb solid solubility.

Construction of Pseudo-Binary Phase Diagram

The basic pseudo-binary phase diagram first drawn by H. L. Eiselstein [2] was modified to include the most recent information. This included the AEM analysis of γ and Laves' phase, and EMP analysis of the eutectic composition by Knorovsky, Cieslak, et. al. [5]. Prinz and Rudolph [4] also added to the diagram with EMP analysis of the solid and liquid phases in the melting range. In support of [4], the % Liquid values from Figure 3 were also used with the Lever Rule to establish the liquidus phase boundary. The contributions of the different researchers are shown in Table II, while the phase diagram construction is shown in Figure 4.

The phase diagram includes a partial nonequilibrium diagram for as-cast Alloy 718 representing a typical segregated casting (or weld), and an equilibrium diagram representing conditions that develop after some homogenization has taken place.

Application of Pseudo-Binary Phase Diagram

The pseudo-binary phase diagram helps to explain several facets observed in typical production experience (paragraph numbers refer to Figure 4):

1. Probably the most frequently encountered mistake during heat treatment or HIP is heating too quickly above 1180C (2150F). Because castings are subject to nonequilibrium solidification, the melting range is extended forcing the solidus boundary to move to the left. This brings the eutectic isotherm at ~1180C (2150F) into an important position. During the original solidification, the liquid with nominally 5 weight percent Cb will be in equilibrium with the first solid to form (the dendrite core, or in the case of Microcast-X the "cell" core). Eiselstein

determined this to be about 4%, but the efforts here and in [4] show it to be closer to 2.0-2.5%. As the solidification temperature drops, the concentration of Cb approaches only 3.5-4.0% probably because 1) carbides tie up some available Cb; 2) the tendency of Cb to partition to the liquid, and; 3) sluggish Cb diffusion in the solid. Thus, a casting with no prior thermal treatments containing a few percent of Laves' phase would be susceptible to melting above 1180C (2150F) if it were heated rapidly, according to the predicted Laves' -> γ + L reaction. One way to avoid melting of this type would be to make sure of adequate temperature control on the heat treatment or HIP furnace to avoid temperature overshoots. Another way is discussed in paragraph #2 below.

2. A slow heating rate between approximately 1065-1180C (1950-2150F) will promote in-situ homogenization. Another technique includes holding below the eutectic isotherm in the range 1150-1163C (2100-2125F) for extended periods of time. This will allow appropriate diffusion of Cb

TABLE II - Contributors To Alloy 718 Pseudo-Binary Phase Diagram

DIAGRAM BOUNDARY	CONTRIBUTOR	TECHNIQUE USED
Eutectic Isotherm Temperature Nonequilibrium Solidus Boundary	[2] [4], This Work	X-ray Diffraction Cb Analysis of Solid by Microprobe, Lever Rule
Liquidus Boundary	[4], This Work	Cb Analysis of Liquid by Microprobe, Lever Rule
Solidus and Liquidus Temperature Maximum Cb Solid Solubility Eutectic Composition Laves' Cb Concentration y Solvus	[4], This Work [5] [5] [5] [2]	Melting Experiments & Metallography Analytical Electron Microscopy Analytical Electron Microscopy Analytical Electron Microscopy X-ray Diffraction

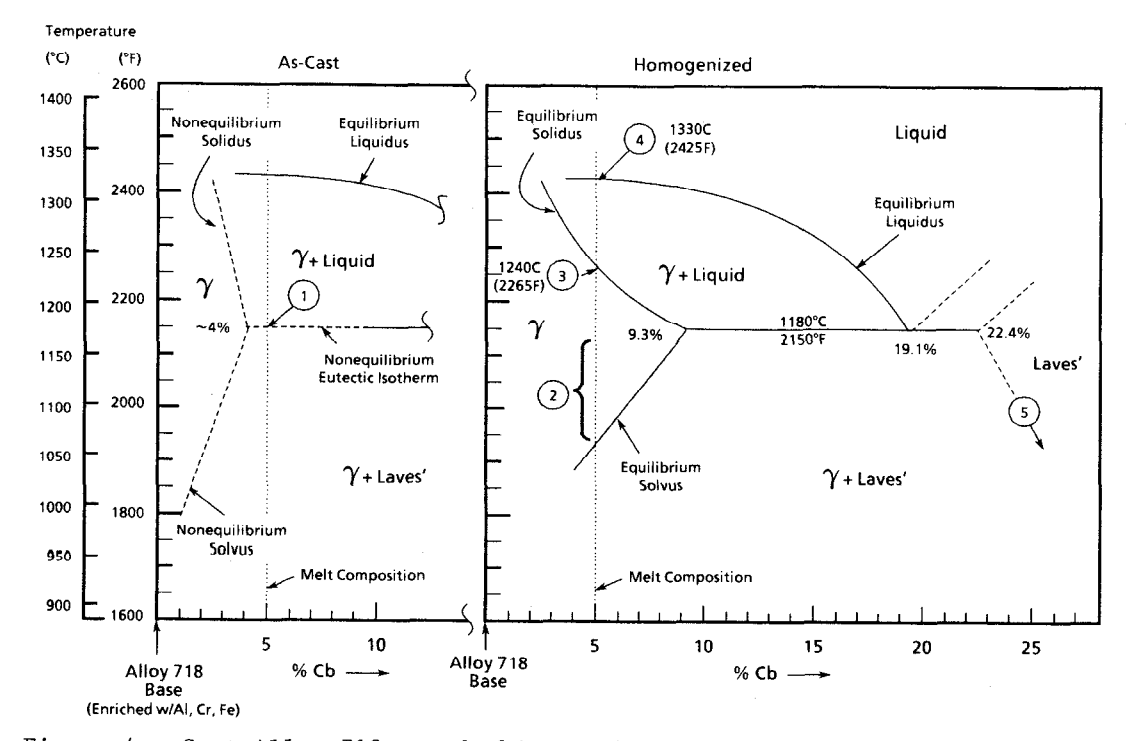


Figure 4. Cast Alloy 718 pseudo-binary phase diagram for the as-cast (segregated) and homogenized conditions. Numbers in circles refer to the text. Constructed from [2,4,5] and this work.

to occur creating the equilibrium phase diagram, as shown to the right in Figure 4. Two examples will be used to confirm the phase boundaries. The first involves a determination of the temperature where Laves' begins to solution in a GTA weld. In the weld metal, Laves' is distributed as small globules which provide a model example for homogenization. The phase diagram predicts that above the solvus, approximately 1060C (1940F), Laves' will begin to dissolve as under equilibrium conditions only γ should be present. In the range of 1065-1095C (1950-2000F), tensile ductility and charpy-impact energy were restored to the GTA welds [8] even though Laves' did not completely dissolve. This indicates that some solutioning occurred. In practice, 1150C (2100F) for one hour was the most practical condition found to dissolve Laves' in GTA welds made on Alloy 718 castings [9].

- 3. Assuming that Laves' phase is sufficiently dissolved, melting will not occur until about 1240C (2265F). In practice this was observed on actual Alloy 718 gas turbine hardware during two HIP runs [9]. At a HIP temperature of 1215 \pm 12C (2220 \pm 25F), near complete solutioning occurred. But with a HIP temperature of 1230 \pm 12C (2245 \pm 25F) the casting began to melt and no solutioning was observed. Thus, at the 1230C (2245F) temperature, it was natural for both solid and liquid phases to coexist.
- 4. As heating continues, the Cb carbides, grain boundaries, and grains begin to melt until complete melting occurs at 1330C (2425F).
- 5. The construction of the Laves' solvus down to ~30% Cb might be contemplated by the reader in an attempt to explain the measured Cb content of Laves' phase, as shown in Table I. Upon cooling from the liquid (as-cast condition), nonequilibrium solidification occurs re-establishing the nonequilibrium phase boundaries, as shown to the left in Figure 4. Just below the eutectic isotherm, there would be two phases coexisting γ and Laves'. The γ would start with a composition of ~4% Cb and the Laves' would start with ~22.4% Cb. As the temperature drops, the composition of γ would follow the γ solvus while the composition of Laves' would follow the Laves' solvus. As it would be simple to extend this boundary down to the measured 30% Cb, this may be incorrect. It is probable that Cb carbides are dissolved within the Laves' phase, which the typical EMP may not be able to distinguish.

SUMMARY

Experiments were conducted to determine the melting range of cast Alloy 718. A new pseudo-binary phase diagram was constructed from several sources to help explain phenomena observed during typical production heat treatments (such as homogenization and HIP). The following guidelines will assist producers and users of cast Alloy 718:

- A. The key to understanding the heat treatment of cast Alloy 718 is to understand Laves' phase. The goal, of course, is to eliminate Laves' phase.
- B. Do not heat the cast product above 1180C (2150F) without some prior homogenization. Doing so will cause incipient melting.
- C. Use slow heating rates approaching the homogenization temperature. Slow rates will promote in-situ homogenization and may prevent incipient melting.

ACKNOWLEDGEMENTS

The author would like to acknowledge helpful discussions with M. Cieslak at Sandia National Laboratory, and M. Kohler of VDM Nickel- Technologie AG. Contributions of several Howmet personnel including the metallographic work of D. Bakos, S. Bellinger, and R. Diehlman, and graphics of M. Stone and M. Behrendt were appreciated. Several discussions with R. Baker, J. Brinegar, L. DePatto, G. Marczak, and P. Merewether of Howmet were also helpful.

REFERENCES

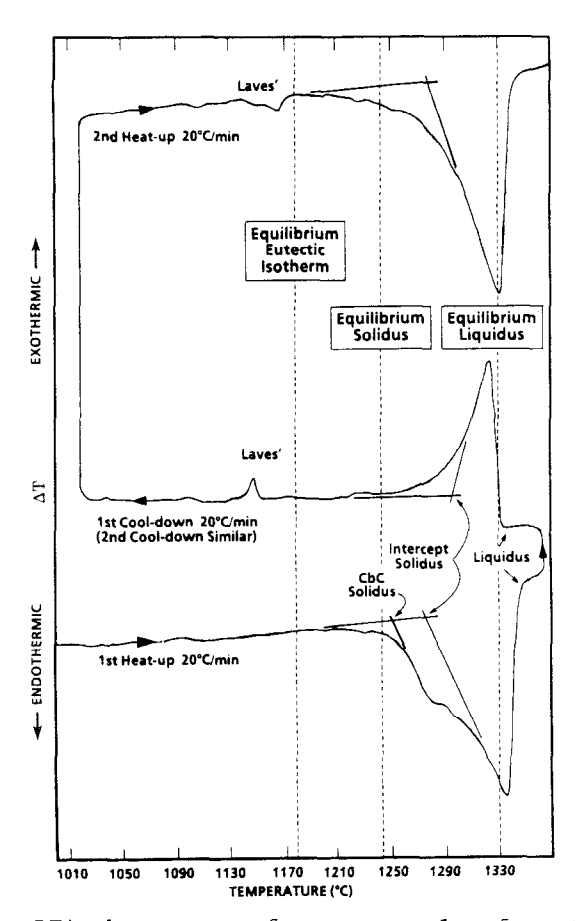
- G. K. Bouse and M. R. Behrendt, "Mechanical Properties of Microcast-X[®] Alloy 718 Fine Grain Investment Castings", this book.
- 2. H. L. Eiselstein, "Metallurgy of a Columbium-Hardened Nickel-Chromium-Iron Alloy", ASTM STP 369 (1965) p62-79.
- 3. F. N. Rhines, Phase Diagrams in Metallurgy, McGraw-Hill, (1956), Ch. 3.
- 4. B. Prinz and G. Rudolph "Microprobe Measurements to Determine the Melt Equilibria of High-Alloy Nickel Materials", Mikrochimica Acta [Wien], Suppl. 11 (1985), p275-287.
- 5. G. A. Knorovsky, M. J. Cieslak et.al., "Inconel 718: A Solidification Diagram", Met. Trans. v20A, in press.
- J. R. Brinegar, K. R. Chamberlain, J. J. Vresics, and W. J. DuPue, United States Patent (Number Forthcoming) "A Method of Forming A Fine-Grained Equiaxed Casting.
- G. K. Bouse and P. W. Schilke, "Process Optimization of Cast Alloy 718 for Water Cooled Gas Turbine Application", ASM, Superalloys 1980 (1980), p303-310.
- 8. J. Gordine, "Some Problems in Welding Inconel 718", The Welding Journal, Nov. 1971, p480s-484s.
- G. K. Bouse and P. W. Schilke, "HTTT Metallurgical Support Investigations of Cast Alloy 718 - Final Report", General Electric Class II Report TR80MPL330, 8/21/80.

APPENDIX - Differential Thermal Analysis (DTA) of Cast Alloy 718

This section was included to compliment our understanding of cast Alloy 718 since DTA is commonly used by industry to characterize melting phenomena. The Microcast-X material used in the main study was heated through the melting range, solidified, melted again, and allowed to solidify a final time. The DTA thermograms are shown in the accompanying figure.

On the 1st heating cycle, the DTA indicates that a transformation has occurred as the curve begins to deviate from the baseline at about 1185C (2165F). This reaction is understood to be the Cb carbides beginning to melt. With an infinitely slow-heating rate, this temperature would probably approach the intercept temperature of 1255C (2290F). As the temperature increases, the bulk of the alloy begins to melt at about 1280C (2335F). The alloy becomes completely liquid at about 1355C (2470F), as indicated by the return of the curve to the baseline.

By comparison to the melting experiments, the dynamic DTA analysis on heating has indicated the solidus and liquidus temperatures have shifted ~35C (63F) higher. As explained earlier, the eutectic isotherm is absent due to the minimal amount of Laves' phase in the sample.



Alloy 718.

On the 1st cooling cycle, the DTA sample has redistributed the alloying elements and produced a slightly different alloy. This casting is unlike the original because of the dendritic grains and the faster solidification conditions. There are several points to consider: 1) The absence of supercooling and/or thermal lag on the liquidus; 2) Decrease in the melting range; 3) Suppression of the CbC peak; and; 4) Formation of Laves' phase. Now there is a sufficient amount of Laves' to produce a peak. If the Laves' liquidus (eutectic isotherm) were interpreted the same way as the alloy liquidus, then the DTA analysis has indicated it is ~35C (63F) lower than predicted by the phase diagram.

On the 2nd heating cycle using the same sample, the Laves' solidus (eutectic isotherm) is comparable to the previous run. This supports the belief that the eutectic isotherm is now lower than it was in the first run. In addition because of the suppressed CbC formation on the 1st cooling cycle, the melting of CbC is no longer detectable. Comparison of DTA thermograms for one sample of cast the alloy solidus and liquidus are also similar to the original heating cycle.

When comparing the 85C (153F) melting range determined by the melting experiments to the DTA cycles, it is clear the true melting range is most accurately described during the heat-up cycle. If the melting carbides could have been removed from the metallographic analyses, then the apparent alloy solidus would have been higher possibly reducing the melting range to ~75C (135F) as recorded by the DTA analyses. Heat-up cycles also present the most consistent picture especially concerning the DTA's characteristic thermal lag. No reasons have been found to explain the narrow melting range recorded by the cooling curves, nor the possible shift in the eutectic isotherm temperature. The one attribute of the cooling curve was the ability to directly interpret the alloy liquidus.

Some reasons for the transformation temperature differences are sensitivity of the DTA instrument (related to sample size among other differences), thermal history of the sample, and of course interpretation. Although the DTA remains a valuable metallurgical tool, it must be used in a consistent manner for reliable and repeatable results.